ICAS-98-7,7,4

A98-31713

NONLINEAR AEROELASTICITY AND FLIGHT DYNAMICS OF AIRCRAFT IN SUBSONIC FLOW

Mayuresh J. Patil* and **Dewey H. Hodges†**
Georgia Institute of Technology, Atlanta, USA

Abstract

Aeroelastic instabilities have always constrained the flight envelope and thus are considered important during design optimization. As we strive to reduce weight and raise performance levels using directional material, thus leading to an increasingly flexible aircraft, there is a need for reliable (less conservative yet accurate) analysis tools, which model all the important characteristics of the Fluid-Structure interaction problem. Such a model would be used in preliminary design and control synthesis. A theoretical basis has been established for a consistent analysis which takes into account, *i)* material anisotropy, *ii)* geometrical nonlinearities of the structure, *iii)* unsteady flow behavior, and *iv)* dynamic stall. The paper describes the formulation for aeroelastic analysis of aircraft with high-aspect-ratio wings. Preliminary results are presented and validated against the exact flutter speed of the "Goland" wing. Further results have been obtained which give insight into the effects of the structural and aerodynamic nonlinearities on the trim solution, flutter speed, amplitude of limit cycle oscillations, and effect of rigid body motion (flight dynamics).

Introduction

The field of aerospace engineering is entering an era of high technology. Over the past decade there has been a great deal of progress in almost all the sub-fields in aeronautics. Control is becoming an integral part of all the sub-disciplines, thus leading to areas of research like control of flexible structures, flow control, and fly-by-wire concept. Also with the rise in the modeling accuracy and production reliability, the designer is approaching what could be called an absolute limit. Optimization is the center of all analysis and design. The aim in all of the above is high performance and safety at a lower cost.

Traditionally, designers sought to optimize the design for individual disciplines. For example, the design of the load-carrying member of a wing was the responsibility of the structural engineer, who had to do it within the constraint of an airfoil shape optimized by an aerodynamacist. The flight control system designer would then work on this design for the best performance and stability norms. Such a design does not always approach the global optimum, the solution to a coupled optimization problem.

Coupled optimization with realistic models is computationally very expensive. One could depend on historical data to constrain the system to the point that it is solvable. An alternative way out is to go for low-order, high-fidelity models which contain most of the higher order/ nonlinear effects and couplings of the aircraft. This would not necessitate constraining of the system, thus leaving it open to newer designs for current flight requirements. Such a system model would also give physical insight into the behavior of the problem, thus highlighting the kind of coupled behavior which is sometimes favorable but can be disastrous at other times.

The last decade has seen an expansion of the flight envelope as well as an increase in the variety of flight missions. Aeroelastic tailoring of composite wings opened an era in which structural coupling was used favorably, making new concepts such as forward swept wings possible. Unmanned aerial vehicles would take the human out of the loop. An increase in flight performance is likely but would have to be accompanied by very robust and intelligent controllers. Here flight maneuvers which were once discarded due to their uncertainties, could be used if the aircraft model (analysis) possesses all the physical characteristics of the aircraft. Then stall could be a regular part of the flight trajectories, and control reversal could be used effectively as

*Graduate Research Assistant, School of Aerospace Engg. Member, AIAA.
†Professor, School of Aerospace Engg. Fellow, AIAA.

21st ICAS Congress
13-18 September 1998
Melbourne, Australia

control augmentation. Again the need is for a model which takes into account the higher-order, nonlinear effects and the various couplings.

Background

Aeroelasticity is a vast field. Aeroelastic instabilities such as divergence and flutter have been the limiting factors for high speed flights. The development of theories for aeroelastic analyses, which started with simplistic models of linear modal analysis for structures and one-dimensional (1-D) quasi steady aerodynamics, have come a long way to the point that tools based on coupling the Finite Element Method (FEM) and Computational Fluid Dynamics (CFD) are in current use. An overview of recent and ongoing research in related fields is presented in detail in an earlier paper.[1]

Aeroelastic analysis of composite wings is a subject of an ever increasing body of literature. The interest stems from the possibility of using directional properties of composites to optimize a wing (i.e., aeroelastic tailoring). Shirk, Hertz and Weisshaar[2] presents a historical background of aeroelastic tailoring and the theory underlying the technology. Librescu and his co-workers were among the first to use a more realistic cross-section; a box beam model made up of various composite laminates for the wing,[3] as opposed to laminated plates. This type of model was analyzed for static aeroelastic instabilities. Banerjee,[4] Chattopadhyay[5] and Patil[6] have investigated the influence of ply angle layup on the static and dynamic aeroelastic characteristics of composite box beams.

Aeroelastic characteristics of highly flexible aircraft is investigated by van Schoor and von Flotow.[7] The complete aircraft was modeled using a few modes of vibration, including rigid-body modes. Waszak and Schmidt[8] used Lagrange's equation to derive the nonlinear equations of motion for a flexible aircraft. Generalized aerodynamic forces are added as closed form integrals. This form helps in identifying the effects of various parameters on the aircraft dynamics.

Nonlinear aeroelastic analysis has gathered a lot of momentum in the last decade due to understanding of nonlinear dynamics as applied to complex systems and the availability of the required mathematical tools. The studies conducted by Dugundji and his co-workers are a combination of analysis and experimental validation of the effects of dynamic stall on aeroelastic instabilities for simple cantilevered laminated plate-like wings.[9] Virgin and Dowell have looked into the nonlinear behavior of airfoils with control surface free-play and investigated the limit-cycle oscillations and chaotic motion of airfoils.[10] On the other hand more insight into nonlinear dynamics itself using nonlinear aeroelastic behavior of an airfoil as an example is investigated by Strganac and co-workers.[11]

The authors[1] have analyzed the nonlinear behavior of cantilevered box beams in subsonic flow. The result include the structural nonlinearities arising due to large displacements and aerodynamic nonlinearities due to stall. Aeroelastic characteristics of the wing were analyzed from the standpoint of stability. A brief description of the models used is presented below. A more detailed formulation of the aeroservoelastic analysis of a complete aircraft is given in an earlier paper by Patil, Hodges and Cesnik.[1]

Formulation

The theory is based on two separate works, viz. *i)* mixed variational formulation based on exact intrinsic equations for dynamics of moving beams,[12] and, *ii)* finite-state airloads for deformable airfoils on fixed and rotating wings.[13, 14] The former theory is a nonlinear intrinsic formulation for the dynamics of initially curved and twisted beams in a moving frame. There are no approximations to the geometry of the reference line of the deformed beam or to the orientation of the cross-sectional reference frame of the deformed beam. A compact mixed variational formulation can be derived from these equations which is well-suited for low-order beam finite element analysis based in part on the original paper by Hodges.[12] The latter work presents a state-space theory for the lift, drag, and all generalized forces of a deformable airfoil. Trailing edge flap deflections are included implicitly as a special case of generalized deformation. The theory allows for a thin airfoil which can undergo arbitrary small deformations with respect to a reference frame which can perform arbitrary large motions.

Structural theory

During the last seven years, a comprehensive framework has been developed for modeling of generally nonhomogeneous, anisotropic beams with arbitrary cross-sectional geometry and material distribution.[15, 16] With the modeling power of the finite element method, it takes a two-step modeling approach which facilitates the accurate treatment of complicated, built-up beam-like structures with a very small number of states. It is based on 3-D elasticity and is capable of modeling complex cross-sectional geometry (solid, built-up, or thin-walled; open or closed; airfoil shaped if necessary),

including all possible couplings and deformation in an asymptotically correct manner.

The framework of structural analysis also gives rise to a set of geometrically-exact nonlinear equations for the beam structural dynamics.[12] Thus, it provides a concise but accurate formulation for handling built-up, beam-like structures undergoing large motions with geometrically nonlinear deformation. It has been successfully applied to rotary-wing static and dynamic aeroelastic stability problems[17] and aircraft composite wing aeroelastic analysis.[1] This formulation is ideally suited for large motion and geometrically nonlinear deformation of wings structures and will be used here. It can be easily augmented to include fuselage motion, by considering the corresponding energies.

The variational formulation is derived from Hamilton's extended principle and can be written as,

$$\int_{t_1}^{t_2} \left[\delta(K-U) + \overline{\delta W}\right] dt = \overline{\delta \mathcal{A}} \tag{1}$$

where K is the kinetic energy of the system, U is the potential energy of the system, $\overline{\delta W}$ represents the virtual work done on the system, $\overline{\delta \mathcal{A}}$ is the virtual action at the end of the time interval, δ is the variational operator, and t_1, t_2 specify the time interval over which the solution is required.

The kinetic energy of the aircraft can be represented as,

$$K = \tfrac{1}{2}\int_0^\ell \left(mV^TV - 2m\Omega\tilde{V}\xi + \Omega^T i\Omega\right) dx_1, \tag{2}$$

where m, ξ, i are, respectively, the mass, mass offset, and inertia matrix per unit length, x_1 is the running axial coordinate along the wing, ℓ is the wing length and column matrices V and Ω represent the total velocity and total angular velocity in the deformed frame.

The gravitational potential energy represented by G can be written as

$$G = \int_0^\ell mge_3^T C^{ia}\left(u + C^{aB}\xi\right) dx_1 \tag{3}$$

where C^{ia} and C^{aB} denote the rotation matrices, and i, a, B represent the inertial, aircraft and wing deformed frames.

The strain energy due to elastic deformation of the wing is given by,

$$U = \frac{1}{2}\int_0^\ell \left\{\begin{matrix}\gamma\\ \kappa\end{matrix}\right\}^T [\mathcal{S}] \left\{\begin{matrix}\gamma\\ \kappa\end{matrix}\right\} dx_1 \tag{4}$$

where γ and κ are one-dimensional strain measures, and $[\mathcal{S}]$ is the 6×6 cross-sectional stiffness matrix.

Now taking the variation of individual energies, we get the expressions for momenta and forces. The expressions for linear momentum P, angular momentum H, and internal force and moment, F, M are given by,[17]

$$P = \left(\frac{\partial K}{\partial V}\right)^T = m\left(V - \tilde{\xi}\Omega\right)$$
$$H = \left(\frac{\partial K}{\partial \Omega}\right)^T = i\Omega + m\tilde{\xi}V \tag{5}$$

$$\left\{\begin{matrix}F\\ M\end{matrix}\right\} = \left\{\begin{matrix}\frac{\partial U}{\partial \gamma}^T\\ \frac{\partial U}{\partial \kappa}^T\end{matrix}\right\} = [\mathcal{S}]\left\{\begin{matrix}\gamma\\ \kappa\end{matrix}\right\} \tag{6}$$

The virtual work done on the system can be written as,

$$\overline{\delta W} = \int_0^\ell \left(\delta u^T f + \overline{\delta\psi}^T m\right) dx_1 \tag{7}$$

where f, m are the external force and moment vectors.

Now using the kinematic relationships derived in Hodges,[12] the expressions for the velocities and the generalized strains can be derived.[1]

In the mixed formulation, the variable expressions are enforced as additional constraints using Lagrange multipliers. Denoting the expressions of all the variables by $()^*$, Hamilton's equation becomes,

$$\begin{aligned}\int_{t_1}^{t_2}\Big\{\int_0^\ell \Big[&\delta V^{*T}P + \delta\Omega^{*T}H - \delta\gamma^{*T}F\\ &-\delta\kappa^{*T}M + \delta u^T f + \overline{\delta\psi}^T m\\ &+\delta\gamma^T(F-F^*) + \delta\kappa^T(M-M^*)\\ &-\delta V^T(P-P^*) - \delta\Omega^T(H-H^*)\\ &+\delta F^T(\gamma-\gamma^*) + \delta M^T(\kappa-\kappa^*)\\ &-\delta P^T(V-V^*) - \delta H^T(\Omega-\Omega^*)\Big] dx_1\Big\} dt = \overline{\delta\mathcal{A}}\end{aligned} \tag{8}$$

The expressions for various quantities and their variations can be substituted in the above equations to get a complete expression for the Hamilton's equation.

The external forces and moments in the above expressions are the various loads acting on the aircraft, including aerodynamic and propulsive loads. Propulsive loads will be assumed as given. The aerodynamic loads will be calculated as described in the following section.

Aerodynamic theory

In order to have a state-space representation of the aerodynamic problem with a low number of states, the finite-state aerodynamic theory of Peters and coworkers[13] is a natural choice. It accounts for large frame (airfoil) motion as well as small deformation of the airfoil in this frame, *e.g.*, trailing edge flap deflection. The theory has been extended to include compressibility effects[14], and gives good dynamic stall results when complemented with ONERA stall model.[13]

The aerodynamic loads used are as described in detail in Peters and Johnson.[13] The theory calculates loads on a deformable airfoil undergoing large deformation in a subsonic flow. Certain aerodynamic parameters for the particular airfoil are required and are assumed to be known empirically or through a CFD analysis. The generalized force measures are given as,

$$\begin{aligned}\tfrac{1}{2\pi\rho}\{L_n\} &= -b^2[M]\left\{\ddot{h_n} + \dot{v_n}\right\} \\ &-bu_0[C]\left\{\dot{h_n} + v_n - \lambda_0\right\} - {u_0}^2[K]\{h_n\} \\ &-b[G]\{\dot{u_0}h_n + \bar{u_0}\zeta_n - u_0 v_n + u_0\lambda_0\}\end{aligned} \tag{9}$$

where ρ, b are the air density and semichord respectively, $\dot{h_n}$, v_n are the generalized deformation and velocities, and λ_0 is the inflow. The matrices denoted by $[K]$, $[C]$, $[G]$, $[S]$, $[H]$, $[M]$ are constant matrices.[13]

The inflow is obtained using the finite-state inflow theory.[18] The inflow (λ_0) is represented in terms of N states $\lambda_1, \lambda_2, \ldots, \lambda_N$ as

$$\lambda_0 \approx \frac{1}{2}\sum_{n=1}^{N} b_n\lambda_n \tag{10}$$

where the b_n are found by least square method, and the λ_n are obtained by solving a set of N first-order differential equations[18]

$$\begin{aligned}&\dot{\lambda}_0 - \tfrac{1}{2}\dot{\lambda}_2 + \tfrac{u_T}{b}\lambda_1 = 2\dot{\bar{\Gamma}} \\ &\tfrac{1}{2n}\left(\dot{\lambda}_{n-1} - \dot{\lambda}_{n+1}\right) + \tfrac{u_T}{b}\lambda_n = \tfrac{2}{n}\dot{\bar{\Gamma}}\end{aligned} \tag{11}$$

The airloads and inflow model can be extended to include the effects of dynamic stall by augmenting the model with the ONERA stall model given below.

$$\begin{aligned}L_{T_n} &= L_n + \rho u_T\Gamma_n \\ \ddot{\Gamma_n} + \tfrac{u_T}{b}\eta\dot{\Gamma_n} + \left(\tfrac{u_T}{b}\right)^2\omega^2\Gamma_n &= \\ -\tfrac{\omega^2{u_T}^3\Delta c_n}{b} - \omega^2 e u_T\tfrac{d}{dt}&\left(u_T\Delta c_n\right)\end{aligned} \tag{12}$$

where, Γ_n is the correction to the circulation. The parameters Δc_n, η, ω^2, and e must be identified for a particular airfoil.

The airloads are inserted into the Hamilton's principle to complete the aeroelastic model.

Solution of the aeroelastic system

Coupling the structural and aerodynamics models one gets the complete aeroelastic model. By selecting the shape functions for the variational quantities in the formulation, one can choose between, *i)* finite elements in space leading to a set of ordinary nonlinear differential equations in time, *ii)* finite elements in space and time leading to a set of nonlinear algebraic equations. Using finite elements in space one can obtain the steady-state solution and calculate linearized equations of motion about the steady state for stability analysis. This state space representation can also be used for linear robust control synthesis. Finite elements in space and time are used to march in time and get the dynamic nonlinear behavior of the system. This kind of analysis is useful in finding the amplitudes of the limit cycle oscillations if the system is found unstable.

Thus three kinds of solutions are possible. *i)* nonlinear steady-state solution, *ii)* stability analysis by linearizing about the steady state. *ii)* time marching solution for nonlinear dynamics of the system.

For steady-state and stability analysis, the formulation is converted to it weakest form in space, while retaining the time derivatives of variable. This is achieved by transferring the spatial derivatives of variables to the corresponding variation by integration by parts. Due to the formulation's weakest form, simplest shape functions can be used.[12] With these shape functions, the spatial integration in Eq. (8) can be performed explicitly to give a set of nonlinear equations.[19] These equations can be separated into structural (F_S) and aerodynamic (F_L) terms and written as

$$F_S(X, \dot{X}) - F_L(X, Y, \dot{X}) = 0 \tag{13}$$

where X is the column matrix of structural variables and Y is a column matrix of inflow states. Similarly we can separate the inflow equations into an inflow component (F_I) and a downwash component (F_W) as

$$-F_W(\dot{X}) + F_I(Y, \dot{Y}) = 0 \tag{14}$$

The solutions of interest for the two coupled sets of equations (Eqs. 13 and 14) can be expressed in the form

$$\begin{Bmatrix} X \\ Y \end{Bmatrix} = \begin{Bmatrix} \bar{X} \\ \bar{Y} \end{Bmatrix} + \begin{Bmatrix} \check{X}(t) \\ \check{Y}(t) \end{Bmatrix} \tag{15}$$

where ($\bar{}$) denotes steady-state solution and ($\tilde{}$) denotes the small perturbation on it.

For the steady-state solution one gets $\bar{Y}$ identically equal to zero (from Eq. 14). Thus, one has to solve a set of nonlinear equations given by

$$F_S(\bar{X},0) - F_L(\bar{X},0,0) = 0 \tag{16}$$

The Jacobian matrix of the above set of nonlinear equations can be obtained analytically and is found to be very sparse.[19] The steady-state solution can be found very efficiently using Newton-Raphson method.

By perturbing Eqs. (13) and (14) about the calculated steady state using Eq. (15), the transient solution is obtained from

$$\begin{bmatrix} \frac{\partial F_S}{\partial X} - \frac{\partial F_L}{\partial X} & 0 \\ -\frac{\partial F_W}{\partial X} & \frac{\partial F_I}{\partial Y} \end{bmatrix}_{\substack{X=\bar{X} \\ Y=0}} \begin{Bmatrix} \dot{\tilde{X}} \\ \dot{\tilde{Y}} \end{Bmatrix} + \begin{bmatrix} \frac{\partial F_S}{\partial X} - \frac{\partial F_L}{\partial X} & -\frac{\partial F_L}{\partial Y} \\ 0 & \frac{\partial F_I}{\partial Y} \end{bmatrix}_{\substack{X=\bar{X} \\ Y=0}} \begin{Bmatrix} \tilde{X} \\ \tilde{Y} \end{Bmatrix} = \begin{Bmatrix} 0 \\ 0 \end{Bmatrix} \tag{17}$$

Now assuming the dynamic modes to be of the form e^{st}, the above equations can be solved as an eigenvalue problem to get the modal damping, frequency and mode shape of the various modes. The stability condition of the aeroelastic system at various operating conditions (steady states) is thus obtained.

To investigate the nonlinear dynamics of the aircraft a time history of aircraft motion and deformation has to be obtained. To get such a solution space-time finite elements are used. This requires that the formulation be converted into its weakest form in space as well as time. Thus, the spatial and temporal derivatives are transferred to the variations. Again due to the weakest form of the variational statement, constant shape functions are used for the variables, and linear/bilinear shape functions are used for the test functions (variations).[20] With these shape functions, Eqs. 13 and 14 take the form,

$$\begin{aligned} F_S(X_i, X_f) - F_L(X_i, X_f, Y) &= 0 \\ -F_W(X_i, X_f) + F_I(Y_i, Y_f) &= 0 \end{aligned} \tag{18}$$

where subscripts i, f, represent the variable values at the initial and final time. If the initial conditions and time interval are specified, the variable values at the final condition is obtained by solving the set of nonlinear equations.

Preliminary Results

Flutter and divergence results have been obtained for a metallic wing used by Goland,[21] and compared with published results (available for the linear case). The results obtained indicate that the steady-state solution and the eigenvalues can be computed efficiently and are accurate. Time marching scheme based on space-time finite elements was found to be stable. The Goland metallic wing was used as a test case since it is based on a real wing and thus gives a realistic idea of the effect of non-linearities in wings. Aeroelastic tailoring of composite box beam "wing" was conducted in an earlier paper[6] and will not be repeated here.

Test case data

The Goland wing data[21] is reproduced below. Other aircraft data (tail data, fuselage data) was chosen *ad hoc* and appended to the wing model to get a complete aircraft model as described below:

Wing half span = 20 ft
Wing chord = 6 ft
Mass per unit length = 0.746 slugs per ft
Radius of gyration of wing about mass center = 25 % of chord
Spanwise elastic axis of wing = 33 % of chord (from l.e.)
Center of gravity of wing = 43 % of chord (from l.e.)
Bending rigidity (EI_b) = 23.65×10^6 lb ft^2
Torsional rigidity (GJ) = 2.39×10^6 lb ft^2
Tail position = 10 ft behind wing elastic axis
Tail half span = 4 ft
Tail chord = 3 ft
Control surface = 50 % of chord
Mass per unit length (tail) = 0.373 slugs per ft
Radius of gyration of the tail = 25 % of chord
Center of gravity of tail = 50 % of chord (from l.e.)
Mass of fuselage = 149.2 slugs
Radius of gyration of fuselage = 6 ft
Mass offset = 1 ft in ahead of wing elastic axis

The aerodynamic data for the airfoil is obtained by curve-fitting the c_ℓ and c_m data. Fig. 1 shows the plot of the assumed linear and stall data. The coefficients for the dynamic stall model, i.e. η, ω and e for a symmetrical airfoil are given as a function of Δc_ℓ.[1]

As shown in Table 1, the current analysis gives the flutter speed and flutter frequency results to within 1 %

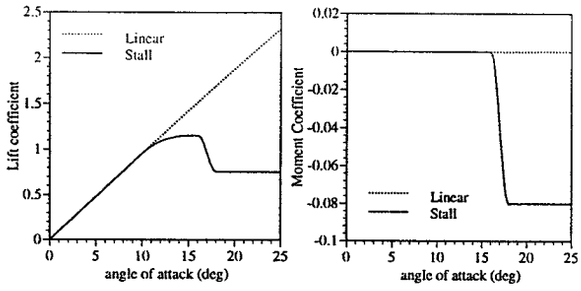

Figure 1: Linear and stall data for c_ℓ and c_m

	Flutter Vel. (ft/sec)	Flutter Freq. (rad/s)
Present Analysis	445	70.2
Exact Solution	450	70.7
Galerkin Solution	445	70.7

Table 1: Comparison of flutter results for Goland wing

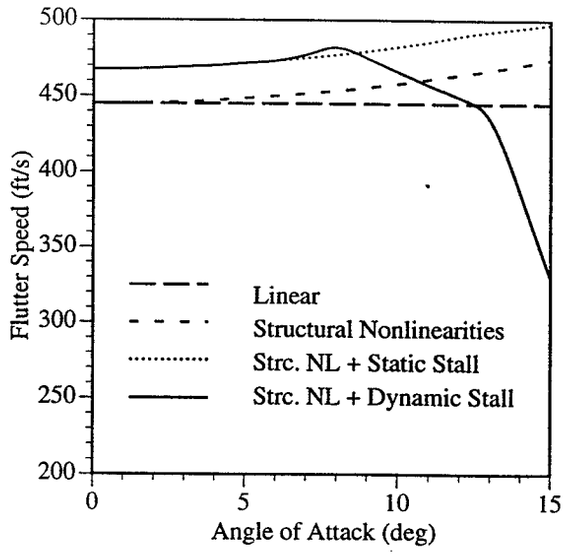

Figure 2: Variation of flutter speed with angle of attack

of the "exact" linear flutter speed of the cantilevered wing.

Effect of nonlinearities on flutter

Structural as well as aerodynamic nonlinearities are known to affect flutter. One of the goals of this research is to be able to determine up front those cases for which nonlinear models are essential for accuracy. As a first step towards that goal, flutter analysis is conducted on the Goland cantilevered wing. The gravitational forces and skin friction drag are neglected in these results. Fig. 2 shows the variation of the flutter speed with increasing angle of attack. The results show the effect of structural nonlinearities, nonlinear static experimental aerodynamic data, and, dynamic stall model on the flutter speed.

As the angle of attack is increased, the aerodynamic load on the wing increases and so do the bending and torsional displacements. The flutter speed is seen to increase due to geometric stiffening. If experimental static aerodynamic data are included in the analysis, then the flutter speed increases even more due to the lower lift-curve slope in the experimental data (i.e., 5.5 as compared to the theoretical value of 2π). Again there is a slight increase in flutter speed with angle of attack due to geometric stiffening. The results including dynamic stall model are markedly different from those without. This is due to coupling between the structural states and the stall states. The stall delay frequency of around 25 rad/sec interacts with the first two structural modes and leads to additional coupling and coalescence, and change in flutter mode. The flutter mode frequency shifts from around 70 rad/sec at 7° to 55 rad/sec at 12°. Also as the angle of attack is increased wing stall occurs at lower speeds thus leading to possibility of flutter at lower speeds.

The effects of structural nonlinearities seem to be small in the above test case which is a low aspect ratio conventional wing. The effects would be considerably higher for a flexible high aspect ratio wings used in UAVs. More work on different models will be presented in a later paper.

Limit cycle oscillations

The flutter results obtained in the earlier section give the velocity of onset of flutter. These flutter results imply that small disturbances will grow exponentially for velocities higher than the flutter speed. But as the amplitude of oscillations grows, so does the additional nonlinear stiffness. Thus, the vibrations do not grow to infinity but instead converge to a limit cycle oscillation (LCO). The amplitude of the LCO gives an idea of the amount of stress/strain on the structure and thus is useful in analysis and design. The amplitude, phase and type of LCO can only be determined by time marching the nonlinear differential equations of motion of the aeroelastic system.

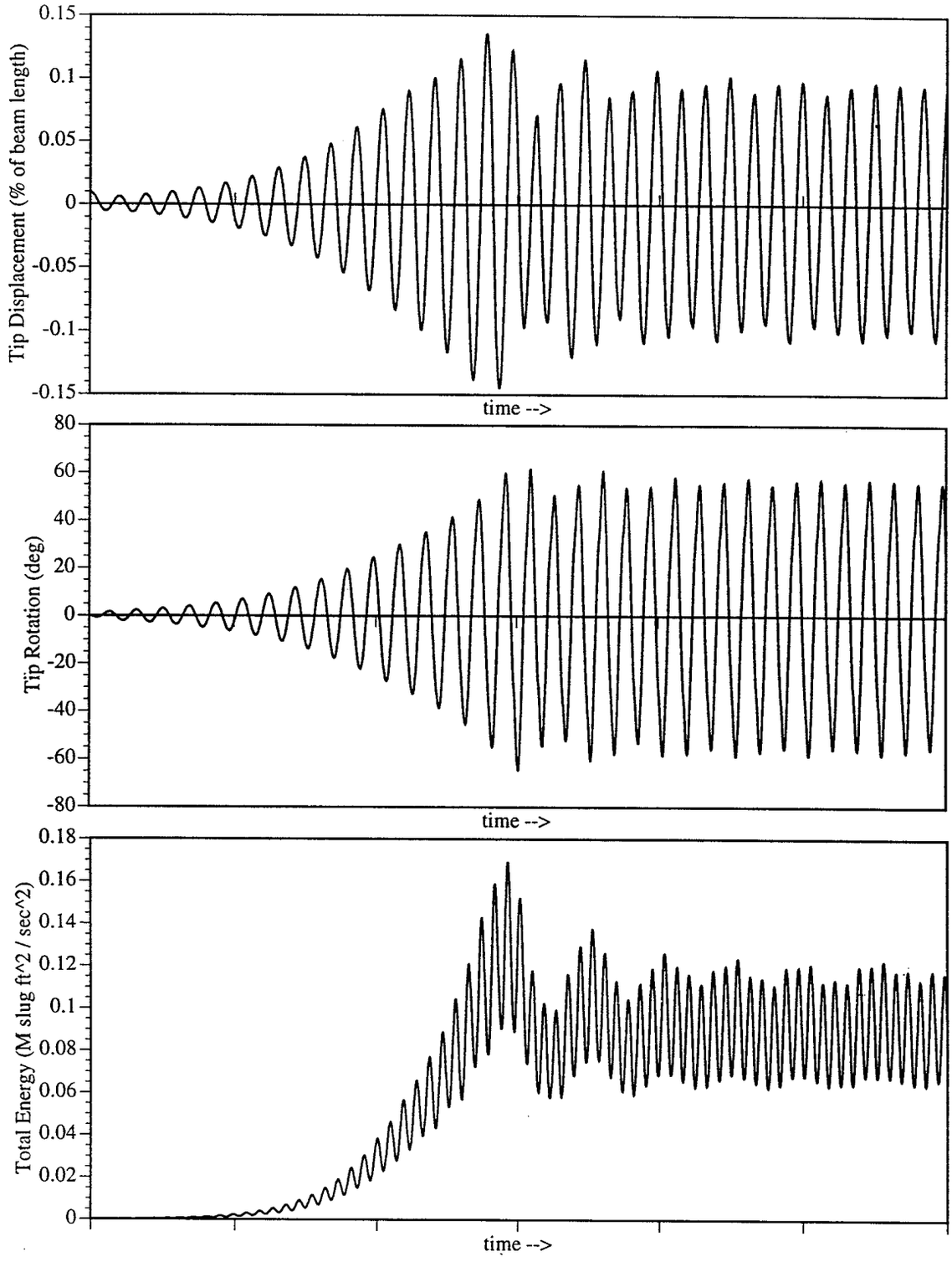

Figure 3: Time history showing LCO above Flutter speed

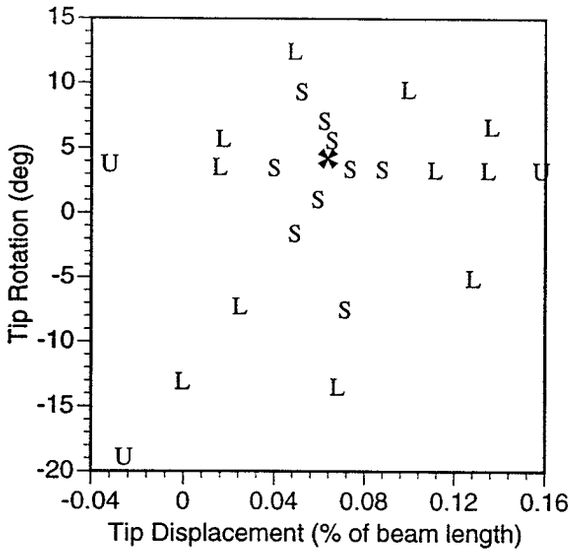

Figure 4: Stability at various Initial conditions

The Goland wing at zero steady-state angle of attack and a velocity of 500 ft/sec ($V_F = 468$ ft/sec) was disturbed by a small disturbance and the time history of oscillations was obtained. The tip displacement, tip rotation and the total energy (sum of kinetic and potential energy) are plotted against time in Fig. 3. The tip displacement and rotation increase exponentially when the amplitude of vibration is small, *i.e.* the nonlinearities are negligible. As the amplitude of vibration increases, nonlinearities due to stall become important and in fact dominant. The aerodynamic forcing function drops and thus can no longer pump the required amount of energy into the structure and the amplitude of oscillation and the total energy levels out.

Another way of looking at the history of oscillations is via a phase plane plot. Here two variables of the system are plotted against each other to give an insight into the modeshape of oscillation. Fig. 5A shows the plot of tip displacement versus tip rotation. One can clearly see the changes in the modeshape as the amplitude increases, and eventually settles into a LCO.

Effect of large disturbances

Stability as calculated by eigenvalues is a linear concept, and thus is valid for small disturbances about the steady state. The flutter speeds calculated above predict that small disturbances grow for speeds higher than the flutter speed and decay for lower speeds. But the disturbances encountered by an aircraft depend completely on its mission and environment, *e.g.* maneuvers, gust amplitudes. A nonlinear system found to be stable under small disturbances may not necessarily maintain stability for higher amplitudes of disturbances. In fact the dynamics of the system can be completely different for varying initial conditions.

Consider the Goland wing at 10° steady-state angle of attack flying with a velocity of 450 ft/sec ($V_F = 466$ ft/sec). Fig. 4 shows the response of the system for various initial conditions. The initial conditions are obtained by deforming the wing with tip forces and moments. "S" denotes a stable response, "L" denotes a a different modeshape which is either a LCO or very lightly damped oscillation, and "U" denotes that the initial modeshape is unstable, and thus the amplitude of ascillation increases and finally settles into a new higher-amplitude LCO. The reason to distinguish between the latter two responses is that the first one has a small amplitude and most likely will not result in structural failure. The above plot shows that depending on the disturbance, the wing may go into a flutter / LCO even at speeds lower than the flutter speed.

The modeshapes in the phase plane are given in Fig. 5. Plot B, shows the behavior of the system for small disturbances. It is lightly damped and the modeshape is that obtained by linear eigenvalue solution. Plots C and D, show the kind of responses for medium level disturbances. The modeshape is nonlinear (non sinusoidal), and depending on the disturbance the damping is either zero or very close to it (C) or small (D). Plots E and F show the initial and final modeshape for high power disturbance. Two plots have been made for easier visualization. Plot E clearly shows that the amplitude of vibration is increasing, and Plot F shows the final converged large amplitude LCO.

Effect of maneuvers

Maneuvers change the system dynamics due to atleast three effects, *i)* system configuration, *ii)* system steady state, *iii)* maneuver induced loads. The system configuration is altered for maneuvers, *e.g.* use of ailerons or spoilers. One would have to do stability analysis for all these configurations. The system steady-state effect is the same as that discussed in the section on the effects of nonlinearities. A high g pull up is such an example. For this maneuver higher lift and thus higher angle of attack would be essential and thus the effects of nonlinearities may become dominant. In the pull up maneuver the wing is also loaded by the g loads but may be small for low ratios of wing to fuselage mass.

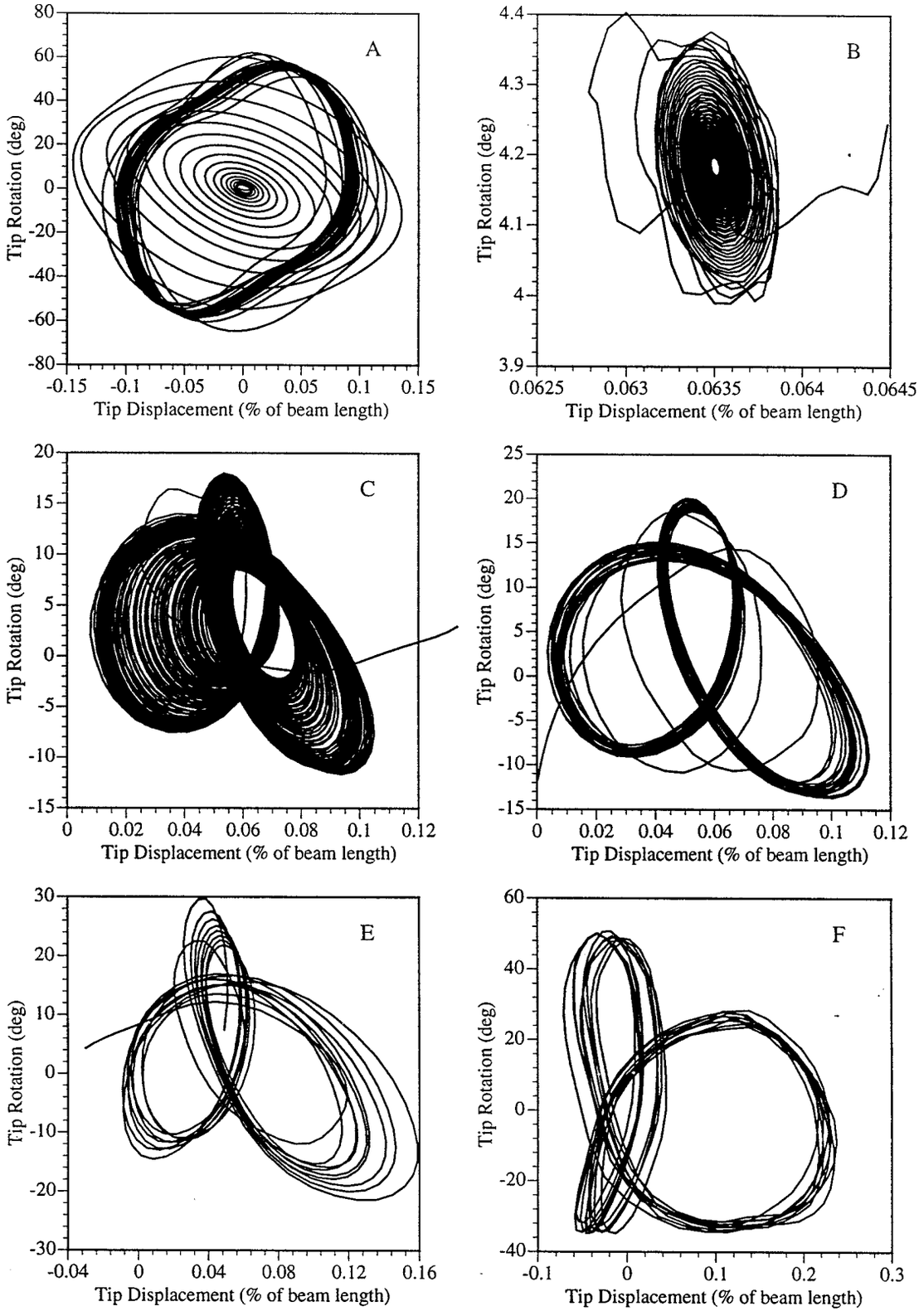

Figure 5: Phase-Plane Diagrams for various Initial Disturbances

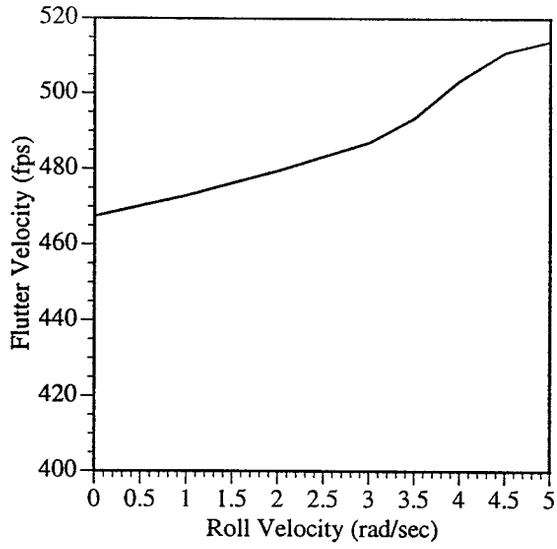

Figure 6: Variation in Flutter Velocity with Roll

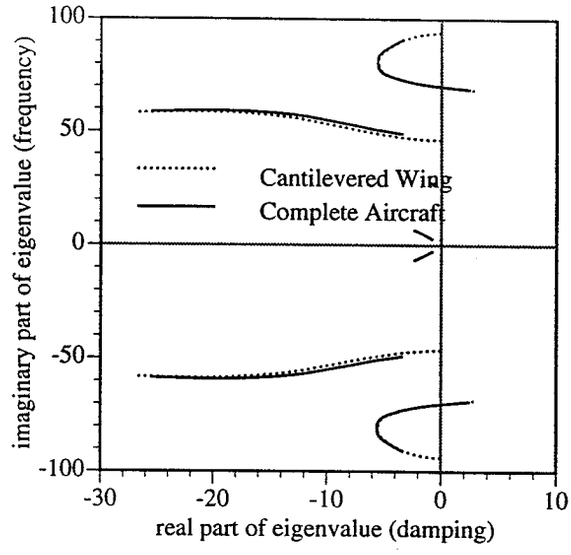

Figure 7: Root locus plot of the aeroelastic aircraft model

Fig. 6 shows the variation of flutter velocity with roll. In a steady roll, centrifugal force induces loads proportional to the distance from the center and thus are high on the wing. This force leads to increased bending stiffness, thus higher flutter velocities.

Effect of rigid-body motion

To quantify the effects of rigid body motion and flight dynamic interactions, the Goland wing model was extended *ad hoc* to create an aircraft model. Fig. 7 shows the root locus plot of some eigenvalues of the system with velocity. There are two sets of curves, one for the cantilevered wing and another for the complete aircraft. Again for the test case one does not see much difference between the two results, except that the phugoid mode is captured if the analysis includes rigid-body modes. One can expect more flight dynamic interactions for a flexible wing where the structural frequencies will be lower and closer to the rigid body frequencies.

Conclusions

A theoretical basis for nonlinear aeroelastic analysis and flight dynamics of aircraft with high-aspect-ratio wings has been presented. It takes into account structural geometric nonlinearities and aerodynamic stall nonlinearities. The equations have been solved using low order finite elements for nonlinear stability analysis. The resulting code has been validated.

Preliminary results are interesting to say the least, and complex at most. The results give deeper insight into effects on nonlinearities on aeroelastic stability. Effect of flight dynamics (aircraft motion) on the aeroelasticity solution, which may involve nonlinear couplings, are also pointed out. The effects of nonlinearities are much higher on a highly flexible wing as opposed to a conventional wing considered here. Once a realistic composite aircraft model is developed, interactions between high flexibility, directional properties and nonlinearities will be modeled and discussed. The effect of flexibility on flight dynamics and control of aircraft is in itself a separate topic and will be discussed in later paper.

References

[1] Patil, M. J., Hodges, D. H., and Cesnik, C. E. S., "Nonlinear Aeroelastic Analysis of Aircraft with High-Aspect-Ratio Wings," In *Proceedings of the 39th Structures, Structural Dynamics, and Materials Conference*, Long Beach, California, April 20 – 23, 1998.

[2] Shirk, M. H., Hertz, T. J., and Weisshaar, T. A., "Aeroelastic Tailoring – Theory, Practice, and Promise," *Journal of Aircraft*, Vol. 23, No. 1, Jan. 1986, pp. 6 – 18.

[3] Librescu, L. and Song, O., "On the Static Aeroelastic Tailoring of Composite Aircraft Swept Wings

Modelled as Thin-Walled Beam Structures," *Composites Engineering*, Vol. 2, No. 5-7, 1992, pp. 497 – 512.

[4] Butler, R. and Banerjee, J. R., "Optimum Design of Bending-Torsion Coupled Beams with Frequency or Aeroelastic Constraints," *Computers & Structures*, Vol. 60, No. 5, 1996, pp. 715 – 724.

[5] Chattopadhyay, A., Zhang, S, and Jha, R., "Structural and Aeroelastic Analysis of Composite Wing Box Sections Using Higher-Order Laminate Theory," In *Proceedings of the 37th Structures, Structural Dynamics, and Materials Conference*, Salt Lake City, Utah, April 1996.

[6] Patil, M. J., "Aeroelastic Tailoring of Composite Box Beams," In *Proceedings of the 35th Aerospace Sciences Meeting and Exhibit*, Reno, Nevada, Jan. 1997.

[7] vanSchoor, M. C. and vonFlotow, A. H., "Aeroelastic Characteristics of a Highly Flexible Aircraft," *Journal of Aircraft*, Vol. 27, No. 10, Oct. 1990, pp. 901 – 908.

[8] Waszak, M. R. and Schmidt, D. K., "Flight Dynamics of Aeroelastic Vehicles," *Journal of Aircraft*, Vol. 25, No. 6, June 1988, pp. 563 – 571.

[9] Dunn, P. and Dugundji, J., "Nonlinear Stall Flutter and Divergence Analysis of Cantilevered Graphite/Epoxy Wings," *AIAA Journal*, Vol. 30, No. 1, Jan. 1992, pp. 153 – 162.

[10] Virgin, L. N. and Dowell, E. H., "Nonlinear Aeroelasticity and Chaos," In Atluri, S. N., editor, *Computational Nonlinear Mechanics in Aerospace Engineering*, chapter 15. AIAA, Washington, DC, 1992.

[11] Gilliatt, H. C., Strganac, T. W., and Kurdila, A. J., "Nonlinear Aeroelastic Response of an Airfoil," In *Proceedings of the 35th Aerospace Sciences Meeting and Exhibit*, Reno, Nevada, Jan. 1997.

[12] Hodges, D. H., "A Mixed Variational Formulation Based on Exact Intrinsic Equations for Dynamics of Moving Beams," *International Journal of Solids and Structures*, Vol. 26, No. 11, 1990, pp. 1253 – 1273.

[13] Peters, D. A. and Johnson, M. J., "Finite-State Airloads for Deformable Airfoils on Fixed and Rotating Wings," In *Symposium on Aeroelasticity and Fluid/Structure Interaction, Proceedings of the Winter Annual Meeting*. ASME, November 6 – 11, 1994.

[14] Peters, D. A., Barwey, D., and Johnson, M. J., "Finite-State Airloads Modeling with Compressibility and Unsteady Free-Stream," In *Proceedings of the Sixth International Workshop on Dynamics and Aeroelastic Stability Modeling of Rotorcraft Systems*, November 8 – 10, 1995.

[15] Hodges, D. H., Atilgan, A. R., Cesnik, C. E. S., and Fulton, M. V., "On a Simplified Strain Energy Function for Geometrically Nonlinear Behaviour of Anisotropic Beams," *Composites Engineering*, Vol. 2, No. 5 – 7, 1992, pp. 513 – 526.

[16] Cesnik, C. E. S. and Hodges, D. H., "VABS: A New Concept for Composite Rotor Blade Cross-Sectional Modeling," *Journal of the American Helicopter Society*, Vol. 42, No. 1, January 1997, pp. 27 – 38.

[17] Shang, X. and Hodges, D. H., "Aeroelastic Stability of Composite Rotor Blades in Hover," In *Proceedings of the 36th Structures, Structural Dynamics and Materials Conference*, New Orleans, Louisiana, April 10 – 12, 1995, pp. 2602 – 2610, AIAA Paper 95-1453.

[18] Peters, D. A., Karunamoorthy, S., and Cao, W.-M., "Finite State Induced Flow Models; Part I : Two-Dimensional Thin Airfoil," *Journal of Aircraft*, Vol. 32, No. 2, Mar.-Apr. 1995, pp. 313 – 322.

[19] Hodges, D. H., Shang, X., and Cesnik, C. E. S., "Finite Element Solution of Nonlinear Intrinsic Equations for Curved Composite Beams," *Journal of the American Helicopter Society*, Vol. 41, No. 4, Oct. 1996, pp. 313 – 321.

[20] Atilgan, A R., Hodges, D. H., Ozbek, A. M., and Zhou, W., "Space-Time Mixed Finite Elements for Rods," *Journal of Sound and Vibration*, Vol. 192, No. 3, May 9 1996, pp. 731 – 739.

[21] Goland, M., "The Flutter of a Uniform Cantilever Wing," *Journal of Applied Mechanics*, Vol. 12, No. 4, December 1945, pp. A197 – A208.